Novel fluorene-based functional 'click polymers' for quasi-solid-state dye-sensitized solar cells†

Md. Anwarul Karim,[a] Young-Rae Cho,[a] Jin Su Park,[b] Sung Chul Kim,[b] Hee Joo Kim,[c] Jae Wook Lee,*[c] Yeong-Soon Gal[d] and Sung-Ho Jin*[b]

Received (in College Park, MD, USA) 7th January 2008, Accepted 6th February 2008
First published as an Advance Article on the web 6th March 2008
DOI: 10.1039/b800032h

Quasi-solid-state DSSCs in SnO_2:F/quasi-solid-state electrolyte/Pt devices have been fabricated with click polymers for the first time; they show a maximum power conversion efficiency (PCE) of 2.80%.

'Click' chemistry has been used extensively since its introduction, due to the high efficiency and technical simplicity of the reaction.[1] Polymer chemists have employed click chemistry to construct dendritic,[2] nonlinear optics,[3] and linear macromolecules.[4] The main obstacles in the synthesis of linear polymers *via* click chemistry are long reaction time and poor product solubility. However, there are only a few reports on the synthesis of π-conjugated polymers by 1,3-cycloadditions,[5] and none was reported in device applications.

As an extension of our previous work,[2] we report the synthesis and characterization of a series of new click polymers (**P1–P4**), which consist of 9,9-dioctylfluorene as a monomer with various types of comonomers such as 4,7-diethynylbenzothiadiazole (**M-3**), *N*-octyl-3,6-diethynylcarbazole (**M-4**), and 9,9-dipropargylfluorene (**M-5**) units. The new polymers (**P1–P4**) were used as a polymer matrix to trap liquid electrolyte to form a quasi-solid-state electrolyte. The dye-sensitized solar cell (DSSC) architecture was SnO_2:F/TiO_2/*cis*-bis(isothiocyanato)-bis(2,2′-bipyridyl-4,4′-dicarboxylato)ruthenium(II) (N3 dye)/quasi-solid-state electrolyte/Pt. The DSSC performance of the above click polymer matrix was also examined for the first time. Scheme 1 shows the structures of **P1–P4** (see ESI† for polymerizations in detail). The molecular structures of the fluorene-based monomers with diazide and diethynyl units are published elsewhere.[5] However, **M-3**, **-4**, and **-5** were used for the first time to synthesize the functional polymers using click chemistry.

The resulting polymers were completely soluble in various organic solvents. Table 1 summarizes the polymerization results, molecular weights, and thermal characteristics of

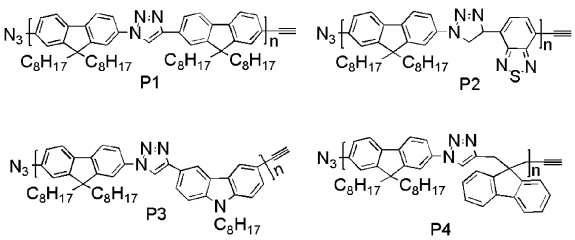

Scheme 1 Molecular structures of click polymers.

P1–P4. The structure and thermal properties of **P1–P4** were identified by ^{1}H-NMR, infrared spectroscopy, elemental analysis, DSC, and TGA thermograms. The disappearance of the characteristics of the acetylenic proton peaks from the monomers at approximately 2.6–3.7 ppm and the appearance of the vinylic proton peaks of the 1,4-disubstituted 1,2,3-triazole ring units in ^{1}H-NMR of **P1–P4** confirmed the polymerization reaction. However, due to the absence of end-capping of the polymer chain, the presence of unreacted alkyne and azide groups in the polymer chain was revealed by the presence of a small band at 2100 cm^{-1} in infrared spectroscopy. The thermal stability of **P1–P4** was determined by TGA under a N_2 atmosphere. As shown in Table 1 (see Fig. S1 in ESI†), isothermal pyrolysis showed that the 1,4-disubstituted 1,2,3-triazole units were lost at approximately 340 °C followed by polymer decomposition at higher temperatures. The glass transition temperatures (T_g) of **P1–P4** ranged from 115–163 °C. It is evident that the incorporation of 1,4-disubstituted 1,2,3-triazole ring units in the main chain can increase the T_g of the resulting fluorene-based polymers. The higher thermal stability of **P1–P4** prevents the deformation and degradation of the active layer by the heat induced during the operation of the devices.

The UV–visible absorption spectra of the polymers **P1–P4**, in solution state, showed absorption maxima at 350, 328, 337, and 323 nm, respectively, as shown in Fig. 1(a). Among the

Table 1 Polymerization results and thermal properties of **P1–P4**

Polymers	Yield (%)	M_w[a] ($\times 10^{-3}$)	PDI[a]	DSC/°C	TGA[b]/°C
P1	92	16	1.92	115	339
P2	90	8.1	1.38	163	323
P3	89	8.6	1.92	148	335
P4	90	33	2.41	135	346

[a] Measured by GPC using polystyrene standards. [b] Measured at temperature of 5% weight loss for the polymers.

[a] *Department of Materials Science and Engineering, Pusan National University, Busan 609-735, Korea*
[b] *Department of Chemistry Education & Interdisciplinary Program of Advanced Information and Display Materials, Pusan National University, Busan 609-735, Korea. E-mail: shjin@pusan.ac.kr; Fax: +82-51-581-2348; Tel: +82-51-510-2727*
[c] *Department of Chemistry, Dong-A University, Busan 604-714, Korea. E-mail: jlee@donga.ac.kr*
[d] *Polymer Chemistry Lab., Kyungil University, Hayang 712-701, Korea*

† Electronic supplementary information (ESI) available: Experimental details, TGA data. See DOI: 10.1039/b800032h

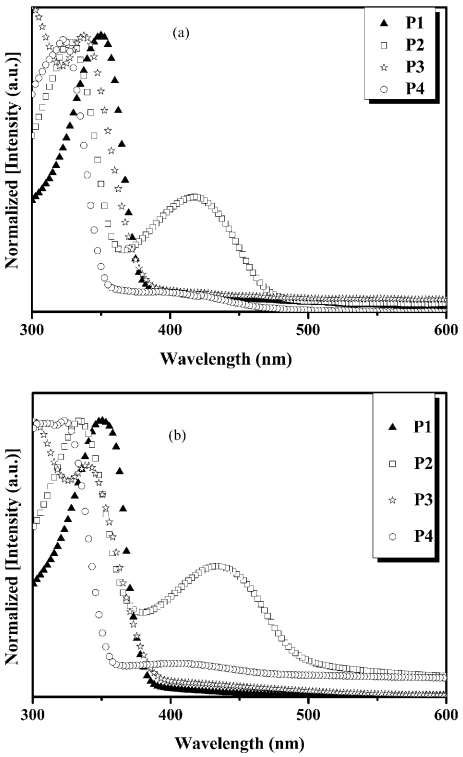

Fig. 1 UV–visible absorption spectra in chloroform (a) and film (b) [concentration: 1.5×10^{-4} M] of **P1–P4**.

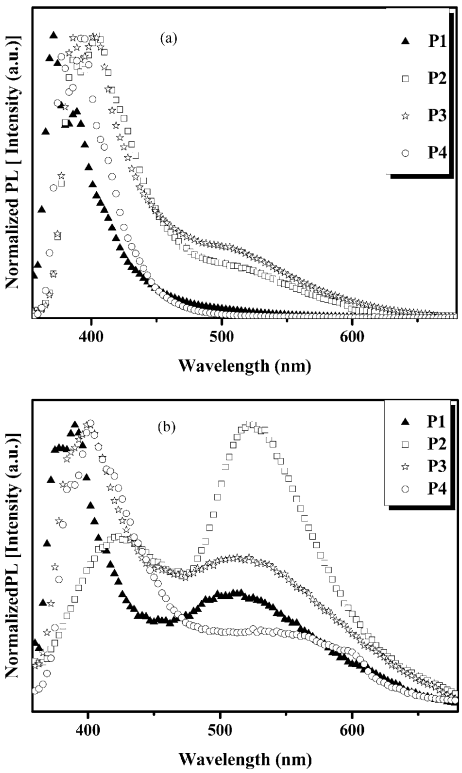

Fig. 2 PL emission in solution (a) and film (b) [concentration: 1.5×10^{-4} M] of **P1–P4**.

polymers **P1–P4**, **P4** showed a significantly enhanced blue shift of its maximum peak in solution when compared with the remaining polymers **P1**, **P2**, and **P3**. This blue shift is consistent with the reduction of the π-conjugated systems induced by the introduction of 9,9-dipropargylfluorene moieties. The polymer **P2** showed two UV–visible absorption peaks at approximately 328 and 434 nm, which were attributed to the introduction of fluorene and benzothiadiazole units along the polymer backbone through the 1,4-disubstituted 1,2,3-triazole linkage.

As shown in Fig. 1(b), the UV–visible absorption spectra of film states were similar to those in solution with a similar maximum absorption wavelength. This indicates a similar conformation of **P1–P4** in both states with tailing structures in the low energy regions in front of steep main absorption band edges.

The PL spectra of **P1–P4** in chloroform were similar and emitted a blue color between 370 and 406 nm as shown in Fig. 2(a), which can be explained using fluorene moiety induced emission bands. These blue bands have well developed vibronic structures with approximately 130 meV vibronic band gaps, which are typical in such π-conjugated systems due to their carbon–carbon double bond stretching mode. These pronounced vibronic structures are common features of both the solution and film PL spectra except for the **P2** film PL spectrum. In addition to these blue bands, **P2** and **P3** have pronounced energetically lower lying structureless bands centered at approximately 525 nm.

This can be explained by the introduction of benzothiadiazole and carbazole moieties with different molecular structures in the polymer chain. As shown in Fig. 2(b), the PL spectra of **P1–P4** in the film states are quite different compared with the solution states. The emission spectra of **P1–P4** in the solid films were slightly red-shifted by 15–40 nm, and had a significantly pronounced energetically lower lying band centered at approximately 525 nm. This red-shift can often be explained by the formation of an interchain excimer. Another possible explanation might be the strong reabsorption due to a relatively steep absorption edge where there is also an emission band for the $S_0 \leftarrow S_1$ 0–0 transition. The most dramatic change was observed in the film PL spectrum of **P2**. The polymer **P2** had a maximum emission peak at 521 nm with a residual blue band at 422 nm, which were attributed to the benzothiadiazole and fluorene units, respectively. This indicates that the electron-deficient benzothiadiazole unit dominates the luminescence properties in its solid state through an energy transfer effect due to the perfectly overlapped blue emission and absorption band centered at approximately 420 nm. In addition, this suggests that the benzothiadiazole containing polymer has the lowest energy level.

Redox measurements were carried out using cyclic voltammetry (CV) to determine the electrochemical properties of **P1–P4** and to evaluate their HOMO and LUMO energy levels. The HOMO binding energies of **P1–P4** with respect to the ferrocene/ferrocenium (4.8 eV) standard were approximately 5.23, 5.39, 5.35, and 4.70 eV for **P1**, **P2**, **P3**, and **P4**, respectively. From the onsets of the absorption spectra, the band gaps of **P1–P4** were calculated to be 3.25, 2.44, 3.14, and 3.46 eV, respectively. The LUMO energy levels were calculated from the band gaps and HOMO energies. It was reported that the HOMO and LUMO energy levels of poly(9,9-

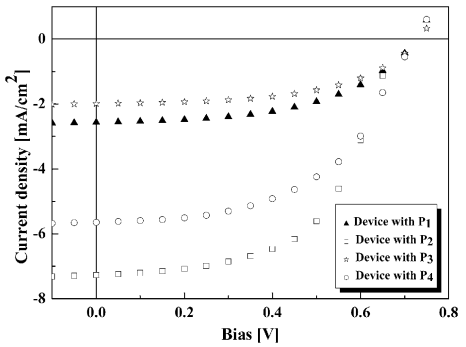

Fig. 3 Photocurrent–voltage characteristics of the DSSCs fabricated with **P1–P4** as a polymer matrix of solid-state electrolyte under AM 1.5 sunlight illumination (100 mW cm^{-2}).

dioctylfluorene) measured using an electrochemical method were 5.8 and 2.12 eV, respectively.[6] There is a significant difference in electrochemical behavior between the reported data and **P1**, which suggests that the electrochemical properties of **P1** had been altered through the introduction of a 1,4-disubstituted 1,2,3-triazole group between the fluorene units along the polymer backbone *via* click chemistry. The LUMO energy level and band gap of **P2** were lower than for the other polymers due to the introduction of electron deficient benzothiadiazole units to the polymer backbone. The HOMO energy level of **P4** was lower than those of **P1–P3** due to the linkage of the dipropargyl unit in its polymer backbone and it facilitates the easy injection of holes from the anode in the PLEDs.

The *J–V* curves of a SnO_2:F/TiO_2/N3 dye/quasi-solid-state electrolyte/Pt device using **P1–P4** as the polymer matrix for the quasi-solid-state electrolyte (see ESI† for device fabrications in detail) under AM 1.5 G illumination (100 mW cm^{-2}) are shown in Fig. 3 and the photovoltaic properties are summarized in Table 2. The absorption characteristics and molar absorption coefficient of the dye or polymer play important roles in determining the performance of the DSSCs. Although dyes such as *cis*-di(thiocyanato)-*N*,*N*′-bis(2,2′-bipyridyl-4-carboxylate-4′-tetrabutylammonium carboxylate)-ruthenium(II) (N719) and N3 showed good dye coverage on TiO_2 and were also reasonably stable, still it has the drawback of low molar absorption coefficients. Relatively high molar absorption coefficients can result in high efficiency because of the extended π-electron delocalization. The values of V_{oc} and FF were similar, which might be due to the triazole linkage at the polymer chain with fluorene as the common repeating unit in **P1–P4**.

Among the four cells, the cell fabricated with **P2** had highest efficiency of about 2.80%. The higher photovoltaic performance of **P2** was due to its low molecular weight and the higher molar absorption coefficient, which allowed the quasi-solid-state electrolyte based on **P2** to easily penetrate the dye adsorbed nanocrystalline porous TiO_2 electrode. Further optimization of the DSSCs through the introduction of crystalline light scattering nanoparticles, the novel processing of mesoporous TiO_2 thin films, and the development of new electrolytes for better DSSC performance is currently underway.

Table 2 Photovoltaic properties of the DSSCs with **P1–P4**

DSSCs with polymers	ε^a /M^{-1} cm^{-1}	V_{oc}/V	J_{sc}/mA cm^{-2}	FF	PCE (%)
P1	430 300	0.72	2.56	0.50	0.96
P2	496 000	0.68	7.27	0.57	2.80
P3	225 400	0.73	1.99	0.54	0.78
P4	485 600	0.72	5.65	0.52	2.12

[a] Measured at a solution concentration 1.0×10^{-5} M.

In conclusion, we were successful in synthesizing a series of novel soluble fluorene-based functional polymers by Cu^{I}-catalyzed 1,3-dipolar 'click chemistry' with reasonable molecular weight. The maximum PCE of the present click polymers was 2.80%, when used as quasi-solid-state electrolyte for DSSCs. This work is expected to provide a new avenue for the application of click polymers in DSSCs, which will facilitate the generation of new functional novel materials in the future.

This work was supported by a Korea Science and Engineering Foundation (KOSEF) grant funded by the Korean government (MOST) (No. M10600000157-06J0000-15710).

Notes and references

1 H. C. Kolb, M. G. Finn and K. B. Sharpless, *Angew. Chem., Int. Ed.*, 2001, **40**, 2004–2021.
2 (*a*) M. Malkoch, K. Schleicher, E. Drockenmuller, C. J. Hawker, T. P. Russell, P. Wu and V. V. Fokin, *Macromolecules*, 2005, **38**, 3663–3678; (*b*) J. W. Lee, B. K. Kim and S. H. Jin, *Bull. Korean Chem. Soc.*, 2005, **26**, 833–836; (*c*) J. W. Lee, B. K. Kim and S. H. Jin, *Bull. Korean Chem. Soc.*, 2005, **26**, 715–716; (*d*) J. W. Lee, J. H. Kim, S. C. Han, W. S. Shin and S. H. Jin, *Macromolecules*, 2006, **39**, 2418–2422.
3 (*a*) Q. Zeng, Z. Li, Z. Li, C. Ye, J. Qin and B. Z. Tang, *Macromolecules*, 2007, **40**, 5634–5637; (*b*) M. Häußler, A. Qin and B. Z. Tang, *Polymer*, 2007, **48**, 6181–6204.
4 (*a*) N. V. Tsarevsky, B. S. Sumerlin and K. Matyjaszewski, *Macromolecules*, 2005, **38**, 3558–3561; (*b*) H. F. Gao and K. Matyjaszewski, *Macromolecules*, 2006, **39**, 4960–4965; (*c*) A. Qin, C. K. W. Jim, W. Lu, J. W. Y. Lam, M. Häussler, Y. Dong, H. H. Y. Sung, I. D. Williams, G. K. L. Wong and B. Z. Tang, *Macromolecules*, 2007, **40**, 2308–2317.
5 (*a*) S. Bakbak, P. J. Leech, B. E. Carson, S. Saxena, W. P. King and U. H. F. Bunz, *Macromolecules*, 2006, **39**, 6793–6795; (*b*) D. J. V. C. Van Steenis, O. R. P. David, G. P. F. Van Strijdonck, J. H. Van Maarseveen and J. N. H. Reek, *Chem. Commun.*, 2005, 4333–4335.
6 S. Janietz, D. D. C. Bradley, M. Grell, C. Giebeler, M. Inbasekaran and E. P. Woo, *Appl. Phys. Lett.*, 1998, **73**, 2453–2455.